Flocculation Kinetics of the Monodisperse System. II. Computer Simulation of Flocculation with Compaction by the Two-Dimensional Geometrical Random Coalescence Model

Yoshihiro AOKI,[a] Yoshiharu YAMADA,*[,b] Kazumi DANJO,[a] Yorinobu YONEZAWA,[a] and Hisakazu SUNADA[a]

Faculty of Pharmacy, Meijo University,[a] Yagotoyama, Tempaku-ku, Nagoya 468, Japan and Central Research Laboratories, Zeria Pharmaceutical Co. Ltd.,[b] Oshikiri, Konan-machi, Osato-gun, Saitama 360-01, Japan.
Received November 21, 1994; accepted March 13, 1995

Computer simulation was carried out to elucidate the growth rate and morphological change of aggregates in flocculation with compaction of monodisperse system by a procedure based on a two-dimensional geometrical random coalescence model. Aggregates were packed closely by partial rotation of the cluster constituting the aggregate when aggregates were flocculated (compaction A) or during measurement of flocculation time (compaction B). Flocculation kinetics were in good agreement with Smoluchowski's flocculation theory. In both compaction methods, the aggregates were packed closely, so that parameters such as the compaction probability and frequency would apply. The aggregates formed by flocculation had hollow structures resembling thick trunks and/or loop structures when they became large. The growth rate of aggregates followed second-order kinetics in both methods. The growth rate constant did not vary with compaction probability in compaction A, but became minimal when the product of compaction probability and compaction frequency was approximately 0.5 in compaction B. Changes in anisometry of aggregates were different for the two methods, that in anisometry simulated by compaction B was more consistent with the data for actual flocculation from a two-dimensional model experiment than change in this parameter simulated by compaction A.

Key words flocculation; agglomeration; computer simulation; aggregate shape; anisometry; particle diameter

An important hurdle in pharmaceutical technology is elucidation of the flocculation mechanism and morphological features of aggregate shapes for suspension of flocculation and granulation. However, it is difficult to directly observe these phenomena in a disperse system owing to the quickness of reactions and delicate experimental conditions. Procedures for theoretical analysis,[1-3] computer simulation[4-16] and model experiment[17,18] must thus serve as the means for analyzing the mechanism of flocculation. Computer simulation was especially useful for maintaining the uniformity of experimental conditions.

The authors previously investigated the kinetics and morphological features of aggregate shapes by cluster–cluster flocculation, whose binding strength between cluster and/or particles was assumed very strong, by computer simulation using a two-dimensional geometrical random coalescence model.[4] In cluster–cluster or cluster–particle flocculation between particles with strong cohesion, aggregate structures became bulky clusters and particles adhered to each other on making contact. The shapes of aggregates reported previously[4] resembled those observed in the model experiment in which agglomerated stearyl alcohol beads flocculated on the surface of water.[17,18]

When an aqueous solution of surfactant was used instead of water, beads constituting an aggregate were seen to become rearranged into a more stable state, that is, compaction. The binding strength between beads in such aggregates was believed to be weak.

As a random addition model,[9-11] there is a simulation procedure dealing with flocculation with compaction. This is the cluster–particle flocculation model, and is considered useful for explaining the layering mechanism. However, Sutherland[12] found the shapes of aggregates obtained with the cluster–particle flocculation model to differ from those obtained with the cluster–cluster flocculation model.

In this study, flocculation with compaction of monodispersed particles was simulated using a modified two-dimensional geometrical random coalescence model as a cluster–cluster simulation procedure. Purpose of the study was to determine the growth rate and morphological changes in an aggregate obtained from flocculation with compaction using the cluster–cluster flocculation model.

Experimental

Flocculation Procedure The procedure essentially is illustrated in Fig. 1, and is the same as a two-dimensional geometrical random coalescence model[4] except for the methods of compaction.

In the initial stage, two-dimensional coordinates with a serial address number from 1 to N_0 ($N_0=4096$, in this study) were assigned and a circle 1.0 unit in diameter as the primary particle was placed on each coordinate to create a monodisperse system. These coordinates did not represent absolute locations of aggregates or particles in a disperse system but the relative locations of particles constituting the aggregate. The center of gravity of the aggregate or particle recorded on a coordinate was thus placed at the origin for convenience of calculation.

Two coordinates with different address numbers were chosen at random using a random number pair (i,j), with i and j between 1 and N_0. When the aggregate or particle was found in both coordinates, the two would approach each other while running parallel to the abscissa, collide and flocculate each other. In compaction A, the flocculated aggregate was packed closely. The new aggregate shape was restored on the i-th coordinate after random rotation using a random number between 0 and 2π, and the aggregate on the j-th one was erased.

When one or both coordinates selected randomly did not have aggregates or particles, another pair of address numbers was chosen. In compaction B, whenever a pair of address numbers was called, a particle making up the aggregate was chosen at random by a random number

* To whom correspondence should be addressed.

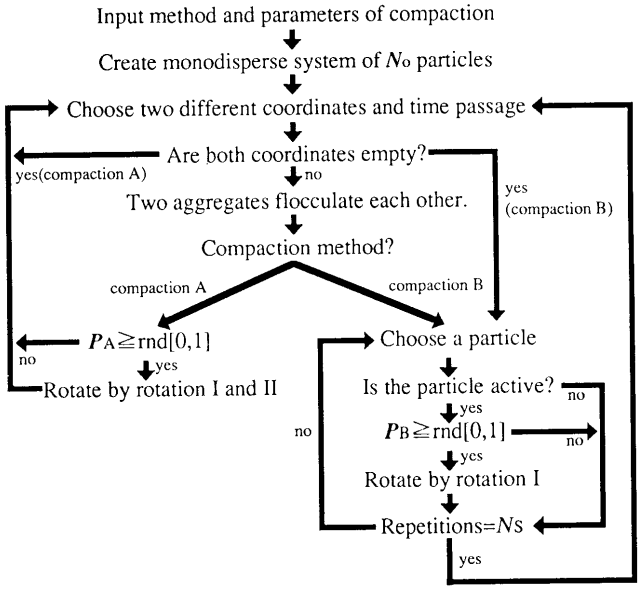

Fig. 1. Flow Sheet of the Simulation Procedure

rnd[0,1] is a random number between 0 and 1.

between 1 to N_0, and then the aggregate was packed closely as described below.

One unit of flocculation time went by for every one hundred pairs of address numbers called. The population numbers and other parameters were printed out at suitable intervals. Calculations were terminated when the number of aggregates in all coordinates became only unity.

Compaction Method Compaction was carried out by partial rotation of an aggregate following compaction A or B set in advance. In these methods, aggregates were packed closely only when the need for compaction was recognized.

Compaction A: The procedure for compaction by partial rotation is illustrated in Fig. 2. When two aggregates i and j collided and flocculated through particles P_i and P_j, respectively, a random number was compared with compaction probability in compaction A P_A set in advance, where the random number and P_A were between 0 and 1. When P_A was larger than the random number, the aggregate i revolved at the center of gravity of P_j until a new collision occurred (rotation I, Fig. 2a). When a new contact particle in the aggregate i was the same as in the case of rotation I, that is, particle P_i, the aggregate i revolved at the center of gravity of particle P_i again (rotation II, Fig. 2b).

An aggregate turned to the direction of the closer distance between the center of gravity of the two aggregates, as shown as Fig. 2c.

Compaction B: One particle in the disperse system was chosen using a random number between 1 and N_0. When the chosen particle was in an aggregate and the aggregate was divided by separating it into more than two aggregates or particles as illustrated in Fig. 3a and b, that is, an active particle,[16] a new random number was generated and compared with the compaction probability of compaction B P_B, where the random number and P_B were between 0 and 1. When P_B was larger than the random number, the aggregate was packed closely according to the procedure for rotation I. In this compaction, rotation II was not carried out because the chosen particles could be selected and packed closely again.

An example of no-chance division of an aggregate, that is, an inactive particle,[16] is shown in Fig. 3c. Compaction was not carried out in this case.

The above compaction procedure was repeated N_S times before a new pair of address numbers was called, N_S being the compaction frequency.

Definition of Diameter, Porosity and Anisometry Diameter D was used as Feret's diameter. Porosity ε reported by Kawashima *et al.*[9] was calculated from the area of a 360-gon inscribed on the periphery of the aggregate and actual projected area. Anisometry Q reported by Medalia[19] was used as the morphological parameter given in Eq. 1,

$$Q = K_A/K_B \tag{1}$$

where K_A and K_B are principal radii of gyration, and equal to half the length of the major and minor axes of the radius-equivalent ellipse, respectively.

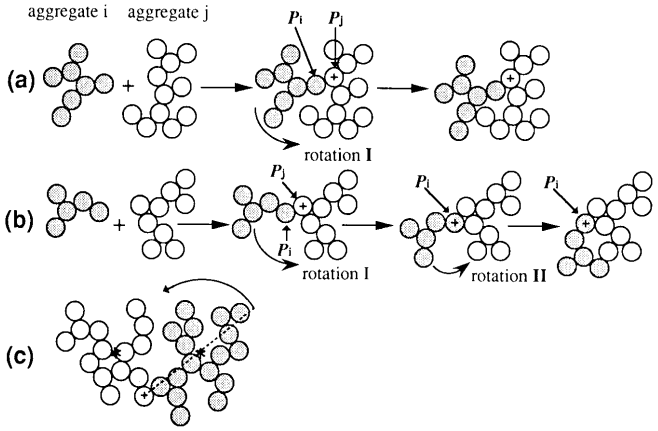

Fig. 2. Procedure for Compaction by Partial Rotation

(a) Only rotation I; (b) rotation I and II; (c) direction of partial rotation. Open and dotted circle clusters show the aggregate i and j, respectively. Plus on a circle and asterisk show the center of revolution and the center of gravity of a cluster, respectively.

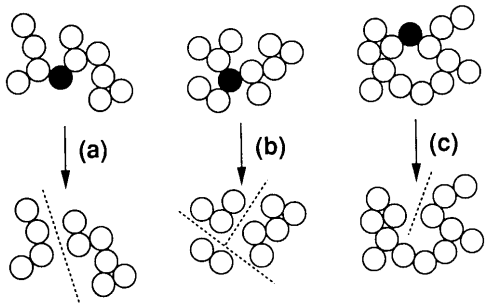

Fig. 3. Definition of Active and Inactive Particle

Closed circles are chosen particles. (a) An active particles divided into two clusters; (b) an active particle divided into three clusters; (c) an inactive particle.

Results and Discussion

Analysis of Flocculation Kinetics Figure 4 shows a typical change in the number of aggregates conforming to the second-order rate Eq. 2,

$$N_0/N - 1 = kN_0t \tag{2}$$

$$t_{1/2} = (kN_0)^{-1} \tag{3}$$

where N is the population number of aggregates or particles at flocculation time t, and k is the flocculation rate constant. $t_{1/2}$ is the half time period of flocculation defined as the flocculation time required for N to become equal to $N_0/2$ (Eq. 3). This figure shows flocculation in this simulation trial to progress by second-order kinetics. k and $t_{1/2}$ in this figure were 5.856×10^{-6} reciprocal unit flocculation time and 41.69 unit flocculation time, respectively.

Smoluchowski provides the following expression for the number of m-fold clusters N_m in fast flocculation,[1]

$$N_m/N_0 = (t/t_{1/2})^{m-1}/(1 + t/t_{1/2})^{m+1} \tag{4}$$

Inserting Eq. 3 in Eq. 2 then gives,

$$N/N_0 = (1 + t/t_{1/2})^{-1} \tag{5}$$

Figure 5 shows population balance of total aggregates, primary particles, and each species up to a cluster 4 times

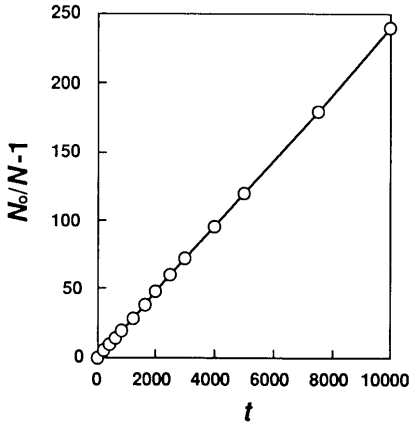

Fig. 4. Applicability of Second-Order Rate Equation of Simulation Results

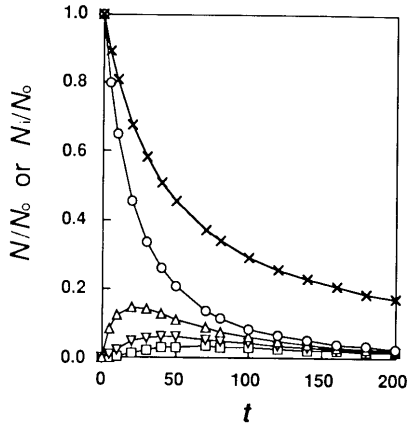

Fig. 5. Smoluchowski Plots of Simulation Results

Population balance of total aggregates ×, primary particles ○, two-fold clusters △, three-fold clusters ▽, four-fold clusters □.

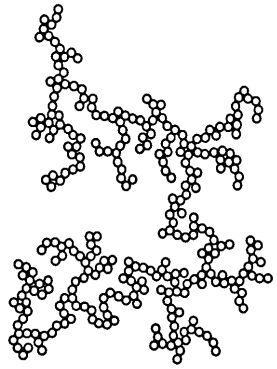

Fig. 6. Typical Simulation Result of Structure of an Aggregate without Compaction

as large as particles as a function of flocculation time. Theoretical curves calculated by Eqs. 4 and 5 using $t_{1/2}=41.69$ unit flocculation time were drawn by solid curves. It is evident from the figure that the simulation model is in agreement with Smoluchowski's flocculation theory.

The compaction methods and compaction parameters such as P_A in the case of compaction A or P_B and N_S in the case of compaction B can change the shapes of aggregates. However, the same results on population kinetics were observed in all simulation trials, since the same procedure for flocculation was used, irrespective of the compaction method and parameter.

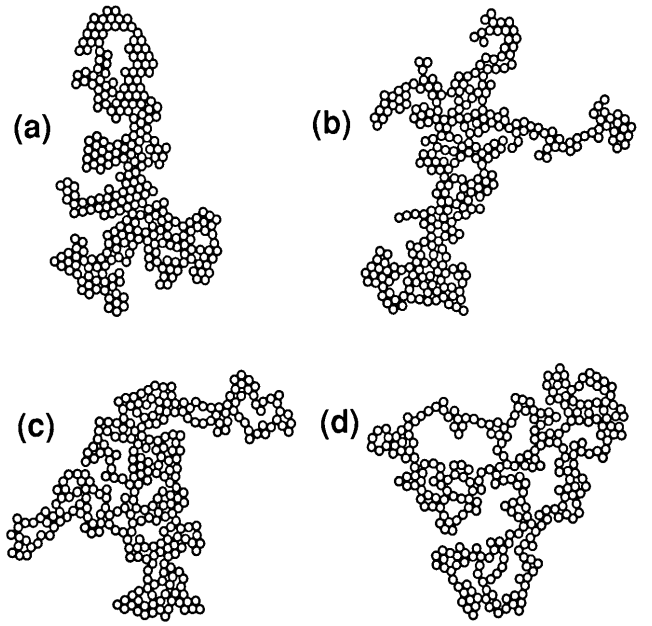

Fig. 7. Typical Simulation Results of Structures of Aggregates with Compaction

Compaction A: (a) $P_A=1.0$; (b) $P_A=0.2$; compaction B: (c) $P_B=1.0$, $N_S=10$; (d) $P_B=0.5$, $N_S=1$.

Comparison of Aggregate Shapes Figures 6 and 7 show typical shapes of aggregates without and with compaction, respectively. Aggregates without compaction had bulky structures, as reported previously.[4] In aggregates from flocculation with compaction, the particles constituting the aggregate were gathered more tightly with increase in compaction parameters such as P_A, P_B and N_S. P_A in the case of compaction A, and P_B and N_S in the case of compaction B may thus change aggregate structures. The aggregates had hollow structures like thick trunks and/or loops after they enlarged; this may have been due to the compaction procedure by partial rotation. When aggregates had hollow structures, they could not be packed more closely.

Effect of Compaction Parameters on Aggregate Growth Changes in mean diameter and porosity of aggregates as a function of flocculation time resulting from compaction A are shown in Fig. 8. The parameters can be seen to increase with flocculation time; the rates of increase in these parameters seem to decrease simply by increasing P_A.

Change in mean diameter and porosity of aggregates in compaction B with flocculation time is shown in Fig. 9. Again, the values increased with flocculation time. From $P_B=0.1$ to $P_B=1$ with $N_S=1$, the rates of increase in mean porosity at the initial stage of flocculation were characteristically faster than in compaction A. Thus compaction parameters control the growth process of aggregates by flocculation with compaction.

Mean porosity seems to converge at infinite flocculation time. Each convergent value should be constant because changes in porosity were controlled by compaction parameters and the initial particle number was constant ($N_0=4096$, in this simulation). Langmuir type equation (Eq. 6) was used to obtain convergent values of aggregate

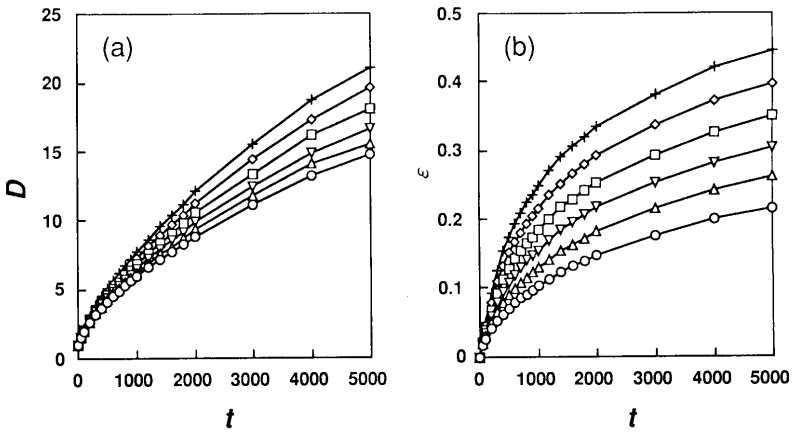

Fig. 8. Mean Diameter and Porosity of Aggregates by Compaction A as a Function of Flocculation Time
(a) Mean diameter; (b) mean porosity: ○, $P_A=1.0$; △, $P_A=0.8$; ▽, $P_A=0.6$; □, $P_A=0.4$; ◇, $P_A=0.2$; +, $P_A=0.0$.

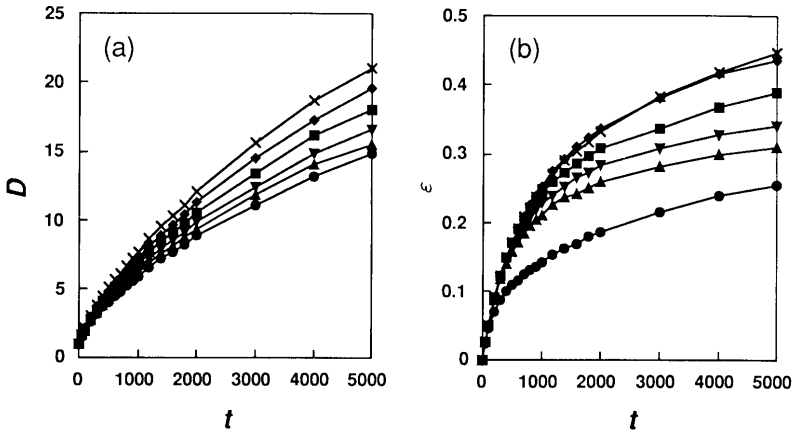

Fig. 9. Mean Diameter and Porosity of Aggregates by Compaction B as a Function of Flocculation Time
(a) Mean diameter; (b) mean porosity: ●, $P_B=1.0$, $N_S=10$; ▲, $P_B=1.0$, $N_S=1$; ▼, $P_B=0.5$, $N_S=1$; ■, $P_B=0.1$, $N_S=1$; ◆, $P_B=0.05$, $N_S=1$; ×, $P_B=0.01$, $N_S=1$.

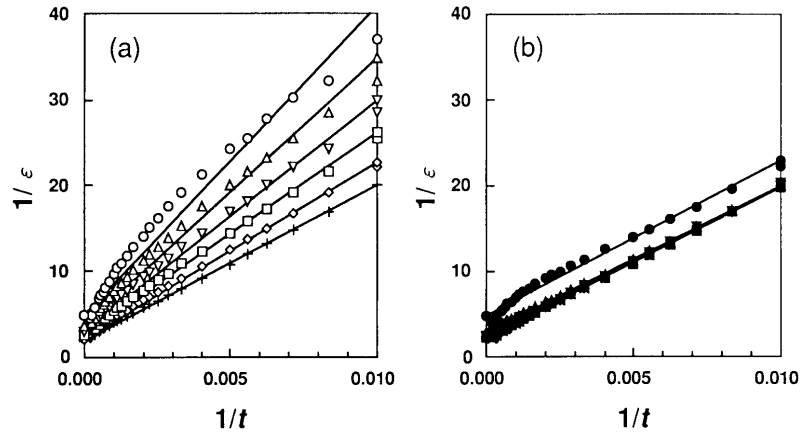

Fig. 10. Relationship between Reciprocal Porosity and Reciprocal Flocculation Time
(a) Compaction A: ○, $P_A=1.0$; △, $P_A=0.8$; ▽, $P_A=0.6$; □, $P_A=0.4$; ◇, $P_A=0.2$; +, $P_A=0.0$; (b) compaction B: ●, $P_B=1.0$, $N_S=10$; ▲, $P_B=1.0$, $N_S=1$; ▼, $P_B=0.5$, $N_S=1$; ■, $P_B=0.1$, $N_S=1$; ◆, $P_B=0.05$, $N_S=1$; ×, $P_B=0.01$, $N_S=1$.

porosity ε_m in both compaction methods,

$$1/\varepsilon = 1/(\varepsilon_m k_P t) + 1/\varepsilon_m \quad (6)$$

where k_P is a constant. These results are shown in Fig. 10. There were differences in slope for compaction parameters in the case of compaction A and no-differences in the case of compaction B. The convergent value of porosity was calculated from reciprocal intercepts of these plots. Relationships between the compaction parameters and convergent values of porosity in both compaction methods are shown in Fig. 11. The product of P_B and N_S as the work index of compaction was used in the case of compaction B. ε_m was inversely proportional to P_A in compaction A. ε_m in compaction B decreased when $P_B \times N_S \leqq 0.05$. P_A and the product of P_B and N_S may thus possibly control compaction conditions of aggregates in each

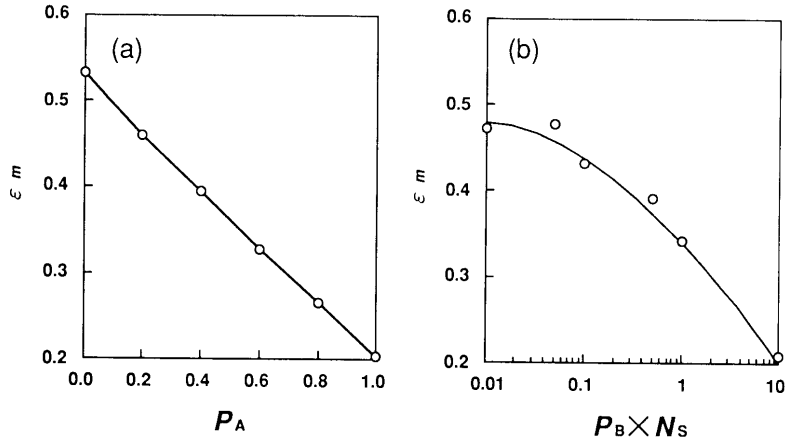

Fig. 11. Relationship between Compaction Parameters and Convergent Porosity
(a) Compaction A; (b) compaction B.

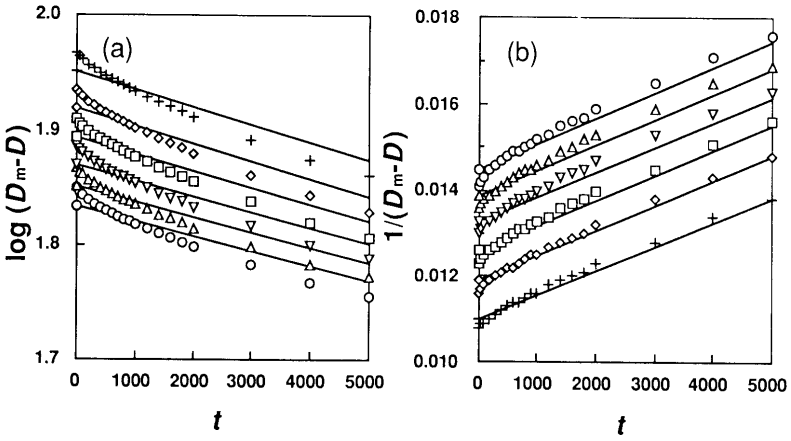

Fig. 12. Applicability of First- and Second-Order Growth Rate Equation to Different Compaction Probability by Compaction A
(a) First-order growth kinetics; (b) second-order growth kinetics: ○, $P_A=1.0$; △, $P_A=0.8$; ▽, $P_A=0.6$; □, $P_A=0.4$; ◇, $P_A=0.2$; +, $P_A=0.0$.

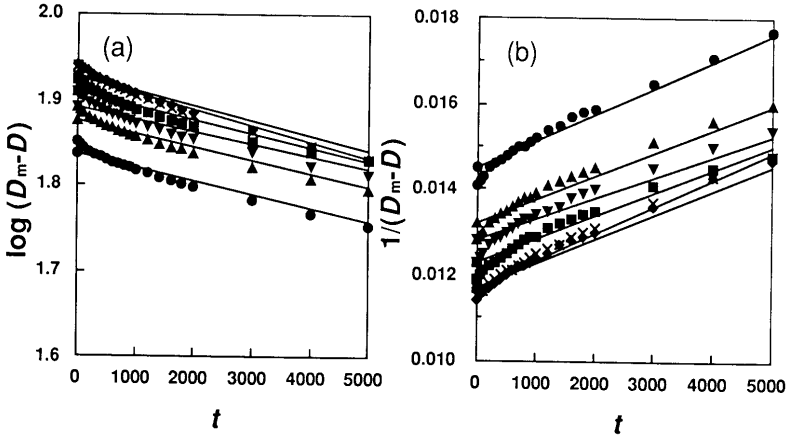

Fig. 13. Applicability of First- and Second-Order Growth Rate Equation to Different Compaction Probability and Frequency by Compaction B
(a) First-order growth kinetics; (b) second-order growth kinetics: ●, $P_B=1.0$, $N_S=10$; ▲, $P_B=1.0$, $N_S=1$; ▼, $P_B=0.5$, $N_S=1$; ■, $P_B=0.1$, $N_S=1$; ◆, $P_B=0.05$, $N_S=1$; ×, $P_B=0.01$, $N_S=1$.

method. The aggregates became more closely with increase in these parameters.

To determine the growth rates of aggregates, the applicability of the first- and the second-order growth rate equations, as expressed in Eqs. 7 and 8, respectively, was investigated (Figs. 12, 13),

$$\log(D_m - D) = k_1 t - \log(D_m) \tag{7}$$

$$1/(D_m - D) = k_2 t + 1/D_m \tag{8}$$

$$D_m = \{4096/(1-\varepsilon_m)\}^{1/2} \tag{9}$$

where D_m is the mean diameter of the maximal aggregate, and defined as the diameter in a circular aggregate con-

Table 1. k_1, k_2 and D_m Values with Various Compaction Parameters

Compaction A						Compaction B						
		First-order rate equation		Second-order rate equation					First-order rate equation		Second-order rate equation	
P_A	D_m	$k_1\times10^5$	r	$k_2\times10^7$	r	P_B	N_S	D_m	$k_1\times10^5$	r	$k_2\times10^7$	r
1.0	71.8	−1.32	0.9889	5.83	0.9977	1.0	10	72.0	−1.58	0.9822	6.15	0.9915
0.8	74.7	−1.35	0.9895	5.81	0.9978	1.0	1	78.9	−1.55	0.9780	5.47	0.9884
0.6	78.0	−1.36	0.9888	5.61	0.9975	0.5	1	82.0	−1.47	0.9688	4.95	0.9810
0.4	82.2	−1.46	0.9907	5.81	0.9980	0.1	1	84.9	−1.63	0.9817	5.39	0.9908
0.2	87.1	−1.53	0.9920	5.86	0.9981	0.05	1	88.5	−1.76	0.9800	5.65	0.9907
0.0	93.6	−1.55	0.9923	5.54	0.9980	0.01	1	88.1	−1.91	0.9901	6.27	0.9970

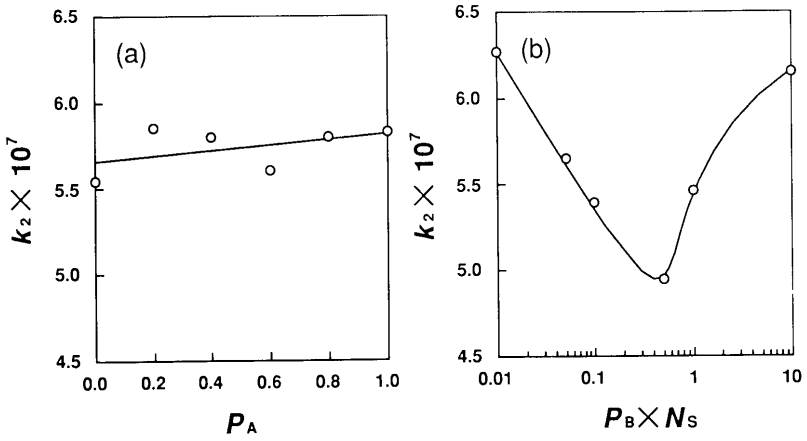

Fig. 14. Second-Order Growth Rate Constant as a Function of Compaction Parameters
(a) Compaction A; (b) compaction B.

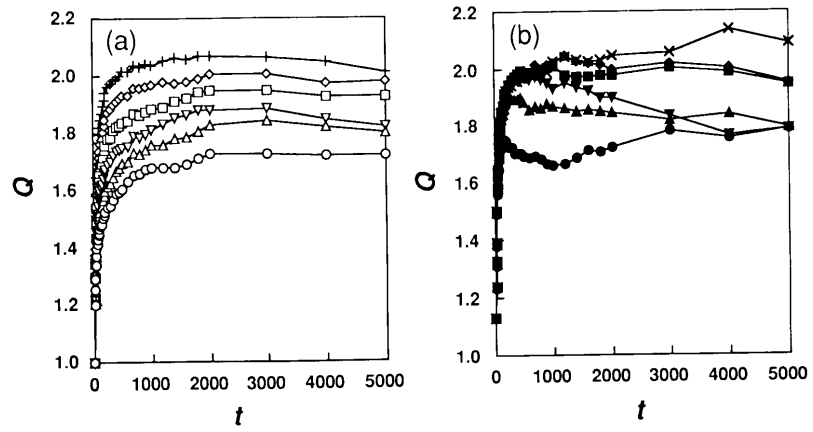

Fig. 15. Mean Anisometry of Aggregates with Compaction as a Function of Flocculation Time
(a) Compaction A: ○, $P_A=1.0$; △, $P_A=0.8$; ▽, $P_A=0.6$; □, $P_A=0.4$; ◇, $P_A=0.2$; +, $P_A=0.0$; (b) compaction B: ●, $P_B=1.0$, $N_S=10$; ▲, $P_B=1.0$, $N_S=1$; ▼, $P_B=0.5$, $N_S=1$; ■, $P_B=0.1$, $N_S=1$; ◆, $P_B=0.05$, $N_S=1$; ×, $P_B=0.01$, $N_S=1$.

sisting of N_0 primary particles and having a void of porosity ε_m. k_1 and k_2 are the first- and second-order growth rate constants, respectively. Table 1 shows values for the maximal diameters, growth rate constants and correlation coefficients r observed in Figs. 12 and 13. From these results, the second-order rate equation showed better fit than the first-order rate equation for both compaction methods. The diameters of aggregates in this simulation trial increased with second-order kinetics.

Figure 14 shows relationships between compaction parameters and second-order growth rate constants calculated by Eq. 8. In the case of compaction A, the growth rate constant k_2 was independent of P_A. k_2 in the case of compaction B was minimum when $P_B\times N_S\fallingdotseq0.5$. The aggregates may thus be packed most efficiently at $P_B\times N_S\fallingdotseq0.5$ and the apparent compaction efficiency may decrease at $P_B\times N_S>0.5$. The apparent compaction probability is thought to have decreased so that the aggregate formed hollow structures when $P_B\times N_S$ was larger than 0.5.

Shapes of Aggregates for Compaction Anisometry Q is a morphological parameter representing the circularity

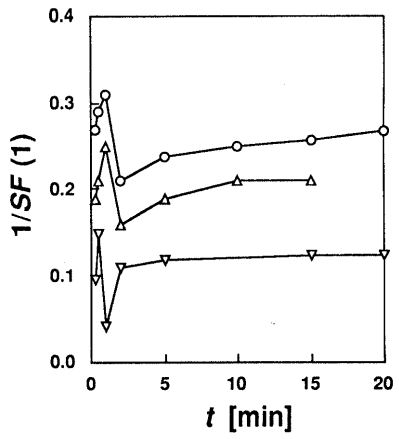

Fig. 16. Reciprocal Shape Factor (1) of Aggregates as a Function of Flocculation Time in Actual Flocculation

Agglomerated stearyl alcohol beads flocculated on the surface of aqueous medium in the presence of sodium lauryl sulfate.[18] $1/SF(1)$ is circularity defined as ratio of the project area of an aggregate to the circle area whose diameter is the longest one in the aggregate. Concentration of sodium lauryl sulfate: ○, 0 w/v%; △, 0.25 w/v%; ▽, 0.50 w/v%.

of an aggregate shape. If the radius-equivalent ellipse reflecting an aggregate shape is similar to a circle, the anisometry is close to 1 and anisometry is larger than 1 in the case of a long ellipse. Figure 15 shows changes in mean anisometry Q of aggregates flocculated by both compaction methods as a function of flocculation time. In compaction A, anisometry increased rapidly at the initial stage of flocculation, and then converged each constant. The constants increased as P_A decreased, due to consumption of primary particles ($Q=1$) and increase in aggregates ($Q>1$).[4] In compaction B, anisometry showed complicated behavior after the initial increase, especially under highly compact conditions. This was believed due to the balance of compaction influence and collision influence. When aggregates are few in the disperse system, collision chance per unit time decreases. The aggregates are packed more closely with flocculation time. However, compaction chance will decrease if active particles are consumed and are not resupplied by new flocculation. When collision influence is larger than compaction influence, anisometry increases and may decrease in the case of larger compaction influence.

These changes in circularity were obtained by the two-dimensional model experiment from agglomerated stearyl alcohol beads on the surface of an aqueous solution of surfactant as shown in Fig. 16, where reciprocal shape factor (1) $1/SF(1)$ is a parameter expressing circularity such as anisometry.[18] The flocculation simulated by the procedure of compaction B can thus be seen to be similar to an actual flocculation.

These simulation methods for flocculation with compaction have a disadvantage such that hollow structures generated by partial rotation are not packed closely again. However, the simulation procedure by compaction B was found more useful for selecting weak bindings in an aggregate and gradual compaction with flocculation time.

References

1) Smoluchowski M., *Phizik. Z.*, **89**, 557, 585 (1916); *idem*, *Z. Physik. Chem.*, **92**, 129 (1917).
2) Müller H., *Koloid-Z.*, **38**, 1 (1926); *idem*, *Kolloidchem-Beih.*, **26**, 257 (1926).
3) Kapur P. C., *Chem. Eng. Sci.*, **27**, 1863 (1972).
4) Yamada Y., Sunada H., *Chem. Pharm. Bull.*, **40**, 1582 (1992).
5) Sunada H., Otsuka A., Yamada Y., Kawashima Y., *Chem. Pharm. Bull.*, **34**, 4308 (1986).
6) Sunada H., Otsuka A., Yamada Y., Kawashima Y., Takenaka H., Carstensen J. T., *Powder Technol.*, **38**, 211 (1984).
7) Sunada H., Otsuka A., Kawashima K., Takenaka H., *Chem. Pharm. Bull.*, **27**, 3061 (1979).
8) Kawashima Y., Takenaka H., Sunada H., Otsuka A., *Chem. Pharm. Bull.*, **30**, 280 (1982).
9) Kawashima Y., Keshikawa T., Takenaka H., Sunada H., Otsuka A., *Chem. Pharm. Bull.*, **30**, 4457 (1982).
10) Sunada H., Otsuka A., Tanaka Y., Kawashima Y., Takenaka H., *Chem. Pharm. Bull.*, **29**, 273 (1981).
11) Kawashima Y., Handa T., Takeuchi H., Niwa K., Sunada H., Otsuka A., *J. Soc. Powder Technol. Jpn.*, **23**, 685 (1986).
12) Sutherland D. N., *J. Colloid Interface Sci.*, **25**, 373 (1967).
13) Meakin P., *J. Colloid Interface Sci.*, **102**, 505 (1984).
14) Meakin P., *J. Chem. Phys.*, **80**, 2115 (1984).
15) Meakin P., *J. Colloid Interface Sci.*, **104**, 282 (1985).
16) Meakin P., *J. Colloid Interface Sci.*, **112**, 187 (1986).
17) Sunada H., Hirai Y., Otsuka A., *J. Soc. Powder. Technol. Jpn.*, **23**, 639 (1986).
18) Sunada H., Takahashi Y., Kurimoto T., Hirai Y., Yonezawa Y., Otsuka A., Kawashima K., *Chem. Pharm. Bull.*, **37**, 3355 (1989).
19) Medalia A. I., *J. Colloid Interface Sci.*, **24**, 393 (1967).